JOURNAL OF MATERIALS SCIENCE 25 (1990) 4822–4827

Preparation of γ-alumina thin membrane by sol–gel processing and its characterization by gas permeation

T. OKUBO, M. WATANABE, K. KUSAKABE, S. MOROOKA
Department of Applied Chemistry, Faculty of Engineering, Kyushu University, 6-10-1, Hakozaki, Higashi-ku, Fukuoka 812, Japan

γ-alumina porous membranes without pinholes or cracks were prepared by the sol–gel process. The boehmite sol obtained from hydrolysation of aluminium isopropoxide was applied to the inner surface of a porous supporting tube by a dipping procedure. The effects of sol concentration and the repetition number of dipping–drying–firing procedure on the membrane performance were investigated by scanning electron microscopy, X-ray diffraction and the Brunauer–Emmett–Teller method in connection with the micro-structure of the membrane. Gas permeation measurements were also conducted. The gas permeation through the thin membranes is well explained by Knudsen's flow, indicating the pores are controlled finely and homogeneously.

1. Introduction

Recently much attention has been focused on inorganic membranes which are superior to organic ones in respect of thermal, chemical and mechanical stability and resistance to microbial degradation. An inorganic membrane can be prepared by various methods such as sol–gel, phase separation and leaching, anodic oxidation, and pyrolysis [1], and disadvantages reported in earlier works are being overcome by the development of novel preparation techniques [2–6].

Usually inorganic films are classified as either nonporous or porous. The former has chemical, mechanical and electrical functions and is used as devices. The latter is mainly used in separation processes where the control of the micro-structure is a key factor. The existence of a pinhole may be fatal to the performance.

The sol–gel process has been applied for the preparation of porous membranes of alumina [2, 3, 7–13], silica [14, 15], titania [10, 12, 13, 16, 17], zirconia [10, 17], ceria [16], ceria–alumina [16] and silica-alumina [4], and has the following features.

1. The thickness of the membrane can be of the order of micrometres.
2. A homogeneous membrane with a large area can be realized.
3. Membranes with a variety of chemical compositions can be prepared.

In this work, a γ-alumina thin porous membrane without pinholes or cracks was prepared by the sol–gel processing, and was characterized by gas permeation as well as structural analyses.

2. Experimental procedure

Boehmite (γ-AlOOH) sol was prepared using the procedure given by Yoldas [18] as shown in Fig. 1. Aluminium isopropoxide (Wako Pure Chemical Industries, Ltd) was used without further purification. To obtain a stabilized sol 0.1 mol HCl per mole boehmite was added, and the boehmite concentration was controlled by evaporation or dilution with distilled water. The aluminium concentration was determined with Inductively Coupled Plasma (ICP) emission spectroscopy (Seiko, SPS1200VR). The particle size distribution of boehmite in the sol was measured by the dynamic light scattering (DLS) method (Otsuka Electronics, DLS-700). The size was expressed in terms of the Stokes diameter.

The membrane was supported on the inner surface of a porous α-alumina tube. The properties of the support tube are summarized in Table I. The pore size distribution determined using mercury porosimetry showed a sharp peak at 1.1 μm. The outer surface of the support tube was wrapped with polyvinylidene chloride film to avoid contact with the sol, and then the tube was dipped in the sol for 10 sec. After the dipping, the membrane was dried overnight in the atmosphere, and then heated to 773 K at 50 K h^{-1}. This dipping–drying–firing procedure was repeated if necessary.

The gas permeation experiment was carried out with helium and nitrogen. The pressure on the outside of the tube (upstream side) was fixed, and the amount of gas permeating to the inner side was determined with a soap-film flow meter. The structure of the

TABLE I Physical properties of support tube

Outer diameter	10 mm
Inner diameter	8 mm
Mean pore diameter	1.1 μm
Porosity	0.43

0022–2461/90 $03.00 + .12

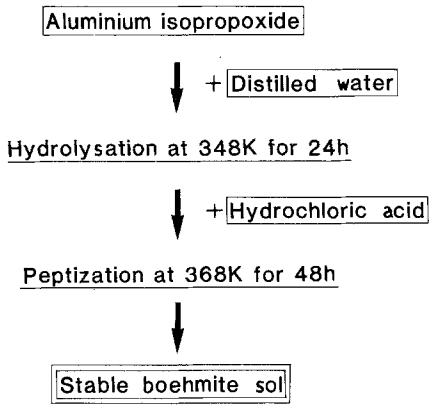

Figure 1 Preparation procedure of boehmite sol.

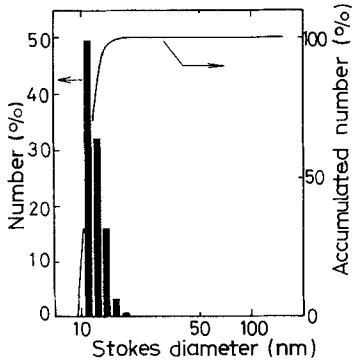

Figure 2 Number-based particle size distribution in original boehmite sol.

membrane was characterized using scanning electron microscopy (SEM), X-ray diffraction (XRD) and Brunauer–Emmett–Teller (BET) adsorption.

3. Results and discussion

3.1. Sol preparation

Fig. 2 shows the number-based particle size distribution in the original sol of concentration 0.52 mol Al/litre. The sol had a sharp peak around ~ 12 nm. The ζ potential was 26.75 mV (Otsuka Electronics, ELS-800), indicating that the particles were positively charged. The XRD (Toshiba, ADG302) pattern of the dried gel (unsupported) with Cu$K\alpha$ radiation revealed that the dispersoid was boehmite, as reported by Leenaars *et al.* [2].

3.2. Structure and morphology of the membrane

Figs 3a and b show the top surface and the fractured section of the membrane observed by SEM (Hitachi, S-2100), respectively. A sol of concentration 0.957 mol Al/litre was used in this case. The boehmite particles were transformed to γ-alumina by firing [2]. Some pinholes exist but no cracks. The surface morphology was not changed by firing. The membranes obtained were 6 μm thick.

Fig. 4 shows the microstructure of the top surface observed by high-resolution SEM (Hitachi, S-900; platinum coating thickness ~ 1 nm). The microstructure was not changed by firing, which indicates the framework of the membrane was constructed in the dipping–drying stage. The membranes were composed mainly of rod-shaped crystallites, as observed by Ono *et al.* [19], with a few plate-shaped ones. This is contrary to Leenaars *et al.* [2] who claimed that their membranes could be modelled as "card packing" of plate-shaped crystallites. As shown in Fig. 4, the pore is about 5 nm in size, and is equivalent to the published data [2, 12, 13].

Particle sizes determined by BET, XRD, SEM and DLS are summarized in Table II. The BET size was calculated assuming spherical particles. The XRD size, D, was obtained from Scherrer's equation [20]

$$D = 0.9\lambda/(B \cos \theta_B) \quad (1)$$

where λ is the wavelength, B the half-width of the peak, θ_B the angle of diffraction. For boehmite particles, the BET and XRD sizes coincided well, while the

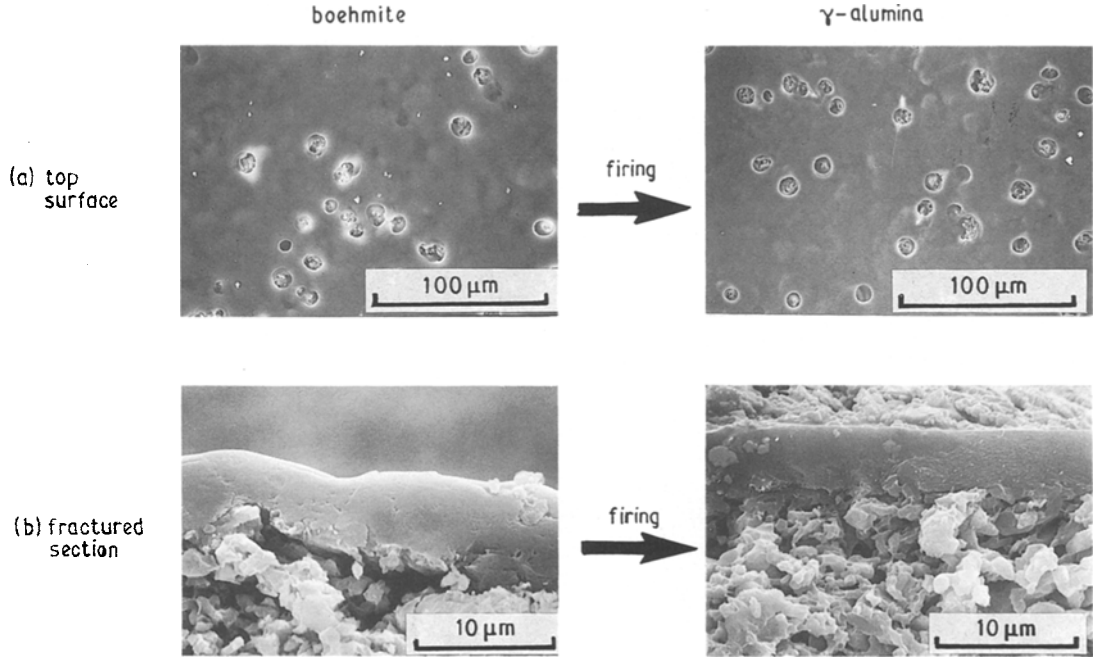

Figure 3 Scanning electron micrographs of (a) top surface and (b) fractured section of boehmite and γ-alumina membranes (sol: 0.957 mol Al/litre).

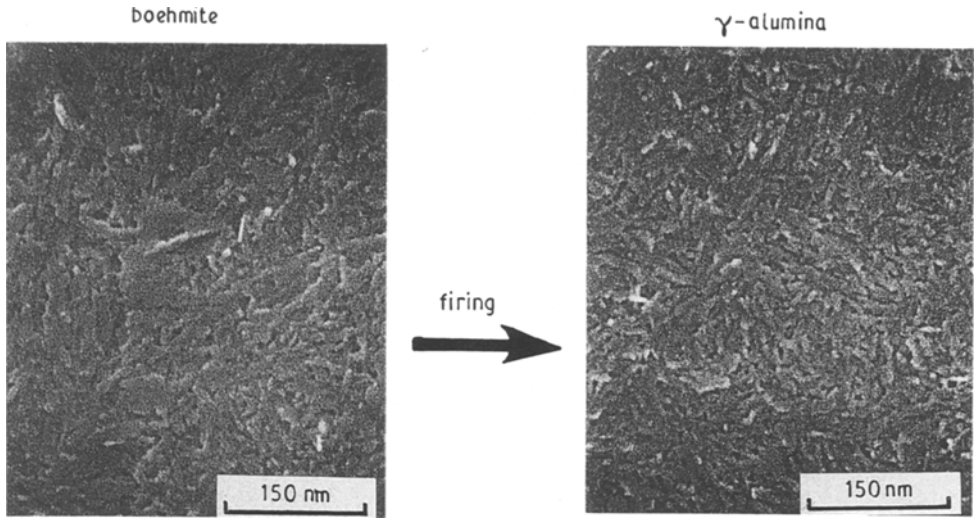

Figure 4 High-resolution scanning electron micrographs (× 200 000) of the top surface of boehmite and γ-alumina membranes (sol: 0.957 mol Al/litre).

DLS gave a slightly larger value. The γ-alumina size obtained was of the same order of magnitude in BET, XRD and SEM. The BET surface areas of the boehmite (before firing) and γ-alumina (after firing) were 523 and 287 $m^2 g^{-1}$, respectively. γ-alumina particles were columnar, 4 nm diameter × 25 nm, and gave a surface area of 292 $m^2 g^{-1}$. This is very close to the measured value.

Fig. 5 illustrates the effect of repeating the dipping followed by firing. Pinholes were clearly covered by the second dipping as indicated by Terpstra *et al.* [9], while the membrane thickness hardly increased. This can be interpreted by a "slip casting" model [3, 21].

3.3. Effect of firing on gas permeability

The permeation rate was determined before and after firing using the 0.815 mol Al/litre sol. The dipping–drying was repeated three times. Fig. 6 shows the effect of the number of dipping times on the permeation rate of helium and nitrogen. The change observed between the second and the third dipping is attributed to the newly formed boehmite layer. The firing process increased the gas permeability in spite of a decrease in the BET area. This may be explained by changes in (1) pore radius, (2) porosity and tortuosity, and (3) membrane thickness. The first factor, however, is rejected because the pore size was not altered by the firing, as shown in Fig. 4. Detailed discussion will be presented in a future publication.

3.4. Effect of repetition of dipping

According to Leenaars and Burggraaf [3], the most important parameters in the dipping procedure were sol concentration, dipping time, pore size of the support, and type and amount of acid used to stabilize the sol. When the green membrane was fired after repeating the dipping–drying procedure more than twice the adhesiveness of the membrane became poor, or the formation of cracks was unavoidable. Therefore, the membrane must be fired after every dipping–drying procedure. It was also found that application of thicker sols resulted in cracking or peeling-off of the membrane during drying. The thickness of the membrane is proportional to the square root of the dip time [3]. This is explained by the slip-casting model [3, 21]. On the other hand, a dilute sol gives no gel layer during dipping, and the pore-clogging process prevails [3, 21]. Then a homogeneous membrane appears after the top surface is flattened. Therefore, application of a dilute sol is effective in preparing a thinner membrane. The sol concentration was thus fixed at 0.52 mol Al/litre for all subsequent experiments.

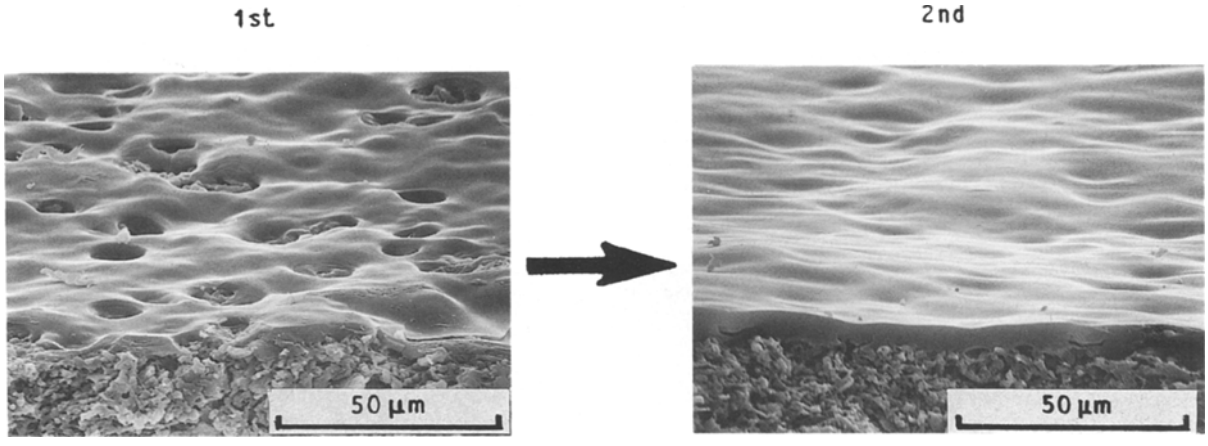

Figure 5 Effect of the second dipping on membrane morphology (sol: 0.957 mol Al/litre).

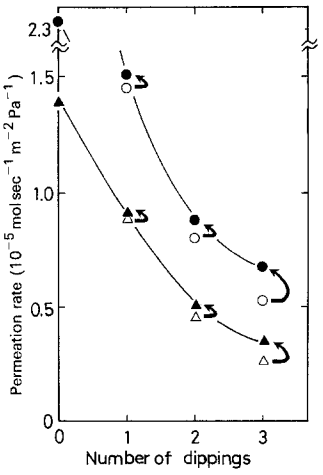

Figure 6 Effect of firing on gas permeation rate at 323 K (sol: 0.815 mol Al/litre). (○, ●) Helium, (△, ▲) nitrogen, (○, △) before firing, (●, ▲) after firing.

Fig. 7 illustrates the effect of repeating the dipping–drying–firing procedure on the total weight of the support and membrane. Each point denotes the average value of 5 to 50 measurements. The increment of membrane weight was larger initially, but was reduced after the fifth repetition.

The gas permeation rate of helium and nitrogen and their ratio are shown in Fig. 8. The permeation rate decreased rather quickly before the fifth dipping, and more slowly after that. The ratio began to rise at the third dipping, and continuously increased with repetition number in this experiment. The morphology of the membranes is illustrated in Fig. 9. Before the fifth dipping, the rough surface of the support was still noticeable, but after the fifth dipping no pinholes or cracks were observed. The increase in the membrane thickness became small after the fifth dipping, and the thickness was 3 μm at this stage. This corresponds to the deceleration of the weight increase shown in Fig. 7. The application of a dilute sol reduced the membrane thickness to the order of the surface roughness of the support. The control of the surface flattening process was a key factor in preparing thinner membranes.

3.5. Gas permeation mechanism through thin membranes

The permeation is affected by the resistances both in the thin membrane and the support. That is, gas molecules pass the support and the thin membrane in series, and the overall permeation rate, $R_{overall}$ can be described as

$$1/R_{overall} = 1/R_{support} + 1/R_{membrane} \quad (2)$$

where R_i denotes the permeation rate through the i-phase. As shown in the previous section, the top surface was homogeneously flattened after the fifth dipping. Therefore, the permeation rate through the membrane dipped five times is defined as $R_{support}$. Using the overall permeation rate through the membranes prepared by ten repetitions of the dipping–drying–firing cycle, the permeation rates through the thin membrane was calculated from Equation 2 to be 2.33×10^{-5} and 9.20×10^{-6} mol sec^{-1} m^{-2} Pa^{-1} for nitrogen and helium, respectively. The permeation ratio was 2.53, which agrees well with the theoretical value based on the following equation [22]

$$R_{He}/R_{N_2} = (M_{N_2}/M_{He})^{1/2} = (28/4)^{1/2} = 2.65 \quad (3)$$

where M_{He} and M_{N_2} denote the molecular weight of helium and nitrogen, respectively. The result implies that gas permeation through the pore in the thin membrane was fundamentally controlled by Knudsen's flow, as suggested from the pore size shown in Fig. 4.

TABLE II Particle sizes determined by different methods

	Boehmite	γ-alumina
BET	D_{sphere} = 3.8 nm	D_{sphere} = 5.6 nm
XRD	D_{120} = 3.8 nm	D_{440} = 3.4 nm
SEM	(not clear)	diameter 4 nm × 25 nm (columnar)
DLS	D_{Stokes} = 12 nm	(not applicable)

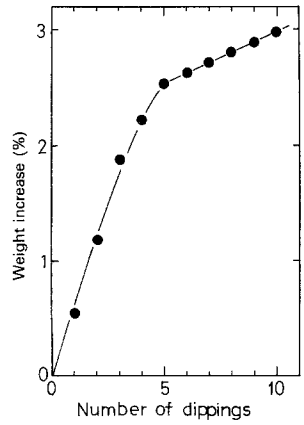

Figure 7 Change in weight increase with repetition of the dipping–drying–firing cycle (sol: 0.52 mol Al/litre).

4. Conclusion

Thin membranes of γ-alumina were produced by sol–gel processing. Pinholes and cracks were covered by repeating the dipping–drying–firing procedure. The

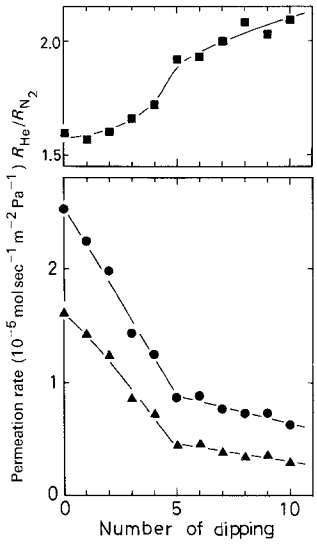

Figure 8 Change in permeation rates of (●) helium and (▲) nitrogen and their ratio at 323 K with repetition of the dipping–drying–firing cycle (sol: 0.52 mol Al/litre).

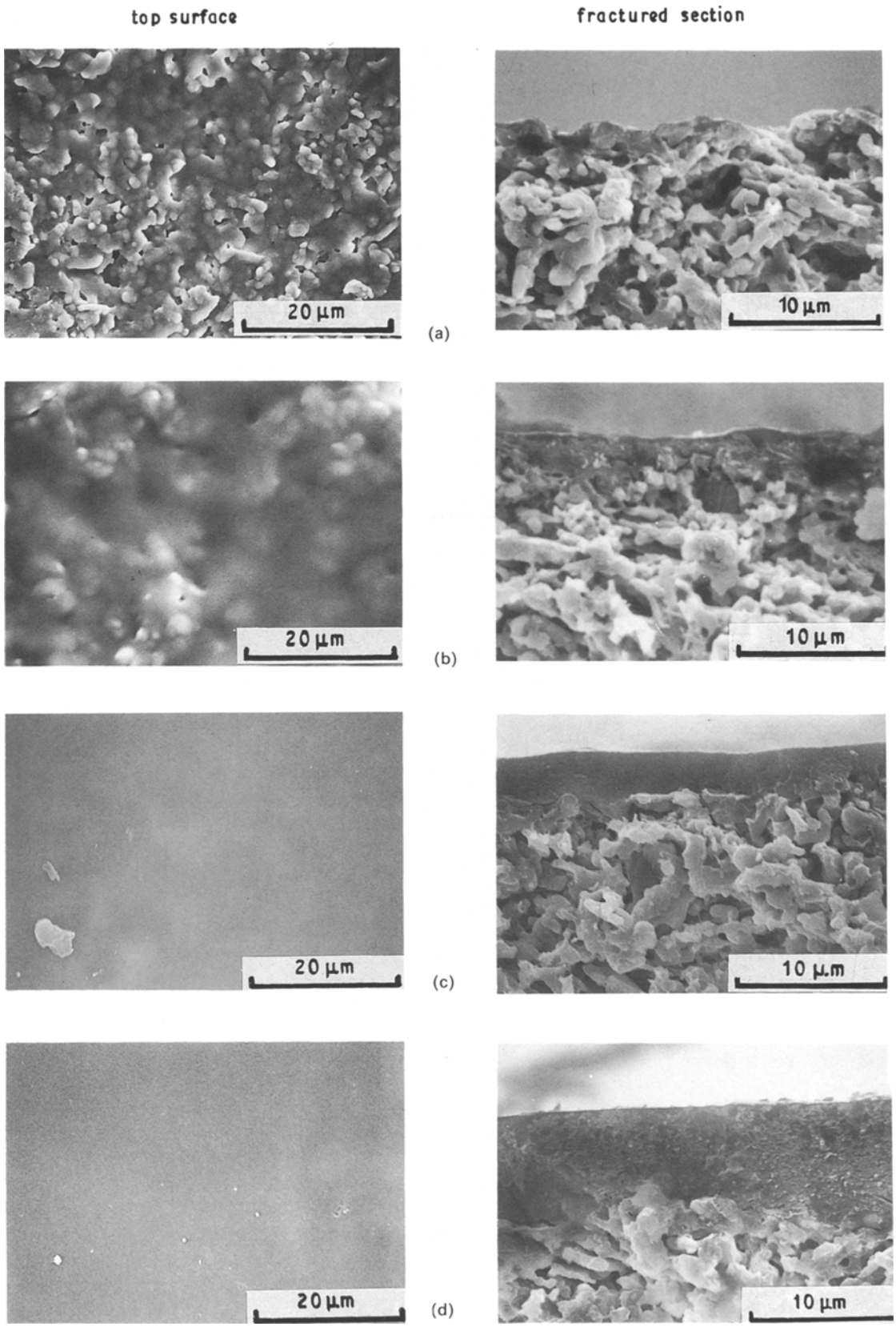

Figure 9 Change in membrane morphology with repetition of the dipping–drying–firing cycle (sol: 0.52 mol Al/litre). (a) Second cycle, (b) fourth cycle, (c) sixth cycle, (d) tenth cycle.

surface morphology and its change on firing were clarified using high-resolution SEM. The pore size of boehmite and γ-alumina membranes was about 5 nm, which was supported by other analyses.

The membrane thickness was 3 μm even after repeating the dipping–drying–firing procedure, when a dilute sol of 0.52 mol Al/litre was used. The surface flattening step was dominant in the initial stage. Permeation of the gas through the thin membrane was mainly controlled by Knudsen's flow mechanism. The selectivity of permeation was in agreement with the theory.

Acknowledgement

The authors thank Hitachi Instrument Engineering

Co. Ltd, Techno-Research Laboratory, Mr T. Suzuki for taking SEM photographs, and Otsuka Electronics for measuring particle size distribution and ζ potential. XRD measurements were taken at the Centre of Advanced Instrumental Analysis, Kyushu University.

References

1. H. P. HSIEH, *AIChE Symp. Ser.* **84** (261) (1988) 1.
2. A. F. M. LEENAARS, K. KEIZER and A. J. BURGGRAAF, *J. Mater. Sci.* **19** (1984) 1077.
3. A. F. M. LEENAARS and A. J. BURGGRAAF, *J. Coll. Interface Sci.* **105** (1985) 27.
4. M. ASAEDA and L. D. DU, *J. Chem. Engng Jpn* **19** (1986) 72.
5. T. OKUBO and H. INOUE, *AIChE J.* **34** (1988) 1031.
6. *Idem, J. Membrane Sci.* **42** (1989) 109.
7. A. F. M. LEENAARS and A. J. BURGGRAAF, *ibid.* **24** (1985) 245.
8. *Idem, ibid.* **24** (1985) 261.
9. R. A. TERPSTRA, B. C. BONEKAMP, H. M. VAN VEEN, A. J. G. ENGEL, R. DE ROOY and H. J. VERINGA, *Sci. Ceram.* **14** (1987) 557.
10. A. LARBOT, J. P. FABRE, C. GUIZARD and L. COT, *J. Membrane Sci.* **39** (1988) 203.
11. H. P. HSIEH, R. R. BHAVE and H. L. FLEMING, *ibid.* **39** (1988) 221.
12. M. A. ANDERSON, M. J. GIESELMANN and Q. XU, *ibid.* **39** (1988) 243.
13. M. J. GIESELMANN, M. D. MOOSEMILLER, M. A. ANDERSON and C. G. HILL Jr, *Separation Sci. Technol.* **23** (1988) 1695.
14. A. KAISER and H. SCHMIDT, *J. Non-Cryst. Solids* **63** (1984) 261.
15. M. NIWA, H. OHYA, Y. TANAKA, N. YOSHIKAWA, K. MATSUMOTO and Y. NEGISHI, *J. Membrane Sci.* **39** (1988) 301.
16. R. J. R. UHLHORN, M. H. B. J. HUIS IN'T VELD, K. KEIZER and A. J. BURGGRAAF, *Sci. Ceram.* **14** (1987) 551.
17. A. LARBOT, J. P. FABRE, C. GUIZARD, L. COT and J. GILLOT, *J. Amer. Ceram. Soc.* **72** (1989) 257.
18. B. E. YOLDAS, *Ceram. Bull.* **54** (1975) 289.
19. T. ONO, Y. OHGUCHI and O. TOGARI, *Stud. Surf. Sci. Catal.* **16** (1983) 631.
20. B. C. CULLITY, "Elements of X-Ray Diffraction" (Addison–Wesley, Reading, Massachusetts, 1956) Ch. 3.
21. D. FREILICH and G. B. TANNY, *J. Coll. Interface Sci.* **64** (1978) 362.
22. E. H. KENNARD, "Kinetic Theory of Gases" (McGraw-Hill, New York, London, 1938) Ch. 2.

Received 11 July
and accepted 1 November 1989